11
Polyoxometalate Nanocapsules: from Structure to Function

Charalampos Moiras and Leroy Cronin

11.1
Introduction

The assembly of nanoscale capsules or cages using metal coordination represents one of the most interesting and challenging areas of chemical nanoscience today. This is because these capsules are composed of many discrete metal- and ligand-based building blocks which have the ability to self-assemble into a single gigantic [1], even protein-sized [2], species, often rapidly and in high yield; most of these have very high symmetry [3], rendering them aesthetically extremely appealing. However, the interest in these systems goes far beyond aesthetics since understanding of the principles and mechanism for the assembly process which leads to their formation will allow systems to be designed from first principles. In this chapter we discuss how polyoxometalate-based molecular capsules and cages are defining a new class of capsules and nanospaces [4]. Nanoscale polyoxometalate clusters (POMs) provide an arguably unrivalled structural diversity of molecules displaying a wide range of important physical properties and nuclearities; these cover the range from 6 to 368 metal ions in a single molecule and are assembled under "one-pot" reaction conditions. At the extreme, these cluster molecules are truly macromolecular, rivaling the size of proteins, and are thought to be formed by a self-assembly process (Figure 11.1) [5]. The clusters are based on metal–oxide building blocks with the general formula MO_x (where M is Mo, W, V and sometimes Nb and x can be 4, 5, 6 or 7). POM-based materials have many interesting physical properties which result from their versatile structures, the ability to delocalize electrons over the surface of the clusters, the ability to incorporate heteroanions, electrophiles and ligands and to encapsulate guest molecules within a metal–oxide-based cage. POM clusters have been shown to exhibit superacidity and catalytic activity [6], photochemical activity [7], ionic conductivity [7] and reversible redox behavior [8]. Therefore, there are many potential applications for this class of molecules [4–8].

Organic Nanostructures. Edited by Jerry L. Atwood and Jonathan W. Steed

ISBN: 978-3-527-31836-0

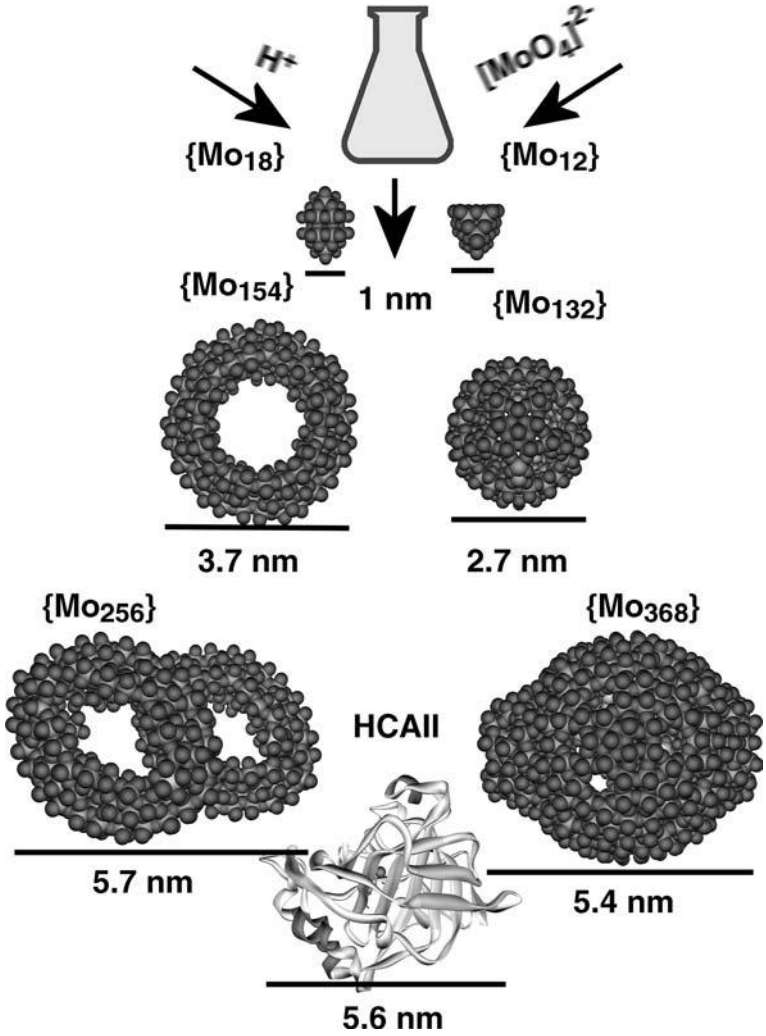

Figure 11.1 Representations of the structures of some POM clusters, all synthesized under "one-pot–one-step" reaction conditions (space filling: Mo large gray spheres, O smaller gray spheres) from the well-known and studied $\{M_{12}\}/\{M_{18}\}$ Keggin–Dawson ions to the $\{Mo_{154}\}/\{Mo_{132}\}$ and $\{Mo_{256}\}/\{Mo_{368}\}$ clusters. These clusters are compared (to scale) with the protein human carbonic anhydrase II (a medium-sized protein with 260 residues, MW 29.6 kDa) to demonstrate their macro dimensions.

Importantly, the assembly of coordination cages involving metal ligand coordination to mediate the self-assembly process depends critically on the building blocks chosen and their respective reactivities. One very important route to the formation of metallosupramolecular architectures involves the selection of building blocks that (1) are preorganized, (2) are kinetically stable, (3) incorporate reactive coordination sites and (4) are complementary. For instance, the exhaustive

study of the molybdenum, tungsten and vanadium oxide systems, i.e. polyoxometalate clusters, has emerged as one of very important and versatile building block source in molecular self-assembly [4,5].

11.2 Background and Classes of Polyoxometalates

The large number of structural types in polyoxometalate chemistry [4,5] can be broadly split into three classes:

1. Heteropolyanions are metal–oxide clusters that include heteroanions such as SO_4^{2-} and PO_4^{3-}. These represent by far the most explored subset of POM clusters, with over 5000 papers being reported on these compounds during the last 4 years alone. There is great emphasis on catalysis in this literature, of which the Keggin $[XM_{12}O_{40}]$ and the Wells–Dawson $[X_2M_{18}O_{54}]$ (where M=W or Mo) anions are fundamental examples. Their popularity, reflected in an enormous volume of literature over several decades, can be attributed to a large extent to the ease of their synthesis or commercial availability, but most importantly to the stability of these clusters. In particular W-based POMs are very stable and this has been exploited to develop W-based Keggin ions with vacancies that can be systematically linked using electrophiles to larger aggregates [4,5].

2. Isopolyanions are composed of a metal–oxide framework, but without the internal heteroatom/heteroanion. As a result, they are often much more unstable than their heteropolyanion counterparts. However, they also have interesting physical properties, such as high charges and strongly basic oxygen surfaces, which means that they are attractive units for use as building blocks [9].

3. Mo-blue and Mo-brown reduced Mo-based POM clusters are related to molybdenum blue-type species, which was first reported by Scheele in 1783 [10]. Their composition was largely unknown until Müller et al. reported, in 1995, the synthesis and structural characterization of a very high nuclearity cluster $\{Mo_{154}\}$ crystallized from a solution of Mo-blue, which has a ring topology [11]. The interest generated by this result is partly due to its high nuclearity and partly because of the size of this cluster; with an outer diameter of ca. 34 Å, an inner diameter of 25 Å and a thickness of 14 Å, it is a truly nanoscopic molecule. Using reaction conditions of pH ≈ 1, with a concentration of Na_2MoO_4 of ca. 0.5 M and a degree of reduction of between 1 and 20%, the solution yields the "giant-wheel" $[Mo_{154}O_{462}H_{14}(H_2O)_{70}]^{14-}$ in over 80% yield in 24 h [12]. The building up principle does not stop there: a series of mixed-valence Mo-blue (containing delocalized Mo^V–Mo^{VI}) clusters (e.g. $[Mo_{256}Eu_8O_{776}H_{20}(H_2O)_{162}]^{20-} \equiv \{Mo_{256}\}$) [13] have been reported and also a class of spherical Mo-brown (containinglocalized Mo^V–Mo^Vunits) clusters (e.g.$[Mo^{VI}{}_{72}Mo^V{}_{60}O_{372}(MeCO_2)_{30}(H_2O)_{72}]^{42-} \equiv \{Mo_{132}\}$) [14] and the highest nuclearity cluster so far found, a "lemon" cluster ($[H_xMo_{368}O_{1032}(H_2O)_{240}(SO_4)_{48}]^{48-} \equiv \{Mo_{368}\}$) [2] (Figure 11.2).

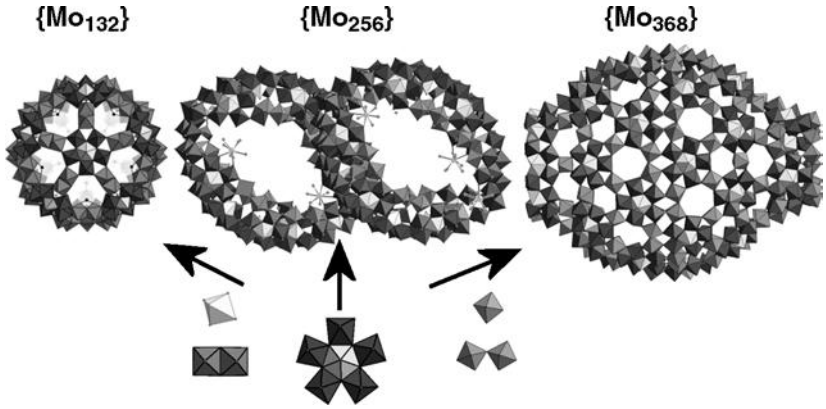

Figure 11.2 Structures of the $\{Mo_{132}\} \equiv [Mo^{VI}{}_{72}Mo^{V}{}_{60}O_{372}(MeCO_2)_{30}(H_2O)_{72}]^{42-}$, $\{Mo_{256}\} \equiv [Mo_{256}Eu_8O_{776}H_{20}(H_2O)_{162}]^{20-}$ and $\{Mo_{368}\} \equiv [H_xMo_{368}O_{1032}(H_2O)_{240}(SO_4)_{48}]^{48-}$ clusters shown with polyhedral plots. The transferable building blocks found in these clusters are shown below also as polyhedral plots whereby the metal is at the center of the polyhedron and the oxygen ligands form the vertexes.

11.3 Wells–Dawson $\{M_{18}O_{54}\}$ Capsules

The Wells–Dawson cluster type can be considered to be an $\{M_{18}O_{54}\}^{m-}$ cluster that often incorporates either one or two templating anionic units e.g. $PO_4{}^{3-}$ and $SO_4{}^{2-}$ [5], so the cluster can be formulated as $([M_{18}O_{54}(XO_n)_2]^{m-}$; M=Mo or W, X = a main group element, $n = 3$ or 4) (Figure 11.3). The $\{M_{18}O_{54}\}^{m-}$ can be considered to have a hydrophilic cavity and can incorporate many types of different anions; traditionally these have been either $PO_4{}^{3-}$ or $SO_4{}^{2-}$ [4,5]. By incorporating electronically interesting anions such as sulfite, it is possible to engineer several types of cluster cage

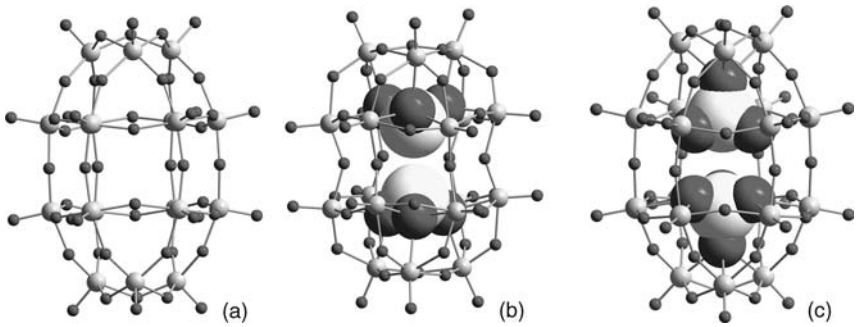

Figure 11.3 Ball and stick representations of (a) $\{M_{18}O_{54}\}^{m-}$, (b) $[Mo_{18}O_{54}(SO_3)_2]^{4-}$ and (c) $[Mo_{18}O_{54}(SO_4)_2]^{4-}$. The M atoms are shown as small gray spheres and the O atoms as dark gray spheres. The S and O atoms of the SO_3 and SO_4 groups are shown in space filling mode.

whereby the anions can themselves interact with each other or undergo reactions inside the cluster cage. This sulfite-containing cluster can be formulated [15] as $[Mo_{18}O_{54}(SO_3)_2]^{4-}$ and the sulfites as positioned within the cluster cage such that they are located only 3.2 Å apart from each other inside the cluster shell (this is 0.4 Å less than the 3.6 Å expected from non-bonded S···S interactions but still longer than the 2.2 Å found in $S_2O_6^{2-}$) and could indicate a strong interaction between the two sulfur atoms; this was also suggested by DFT calculations [15]. In the limit it was thought that engineering such capsules may allow the oxidation of sulfite to yield dithionate $S_2O_6^{2-}$ anions (note: sulfur is the only main group element to form $X_2O_6^{n-}$ analogues with X−X single bonds), e.g.

$$2SO_3^{2-} \rightarrow S_2O_6^{2-} + 2e^-$$

Thus, engineering an intramolecular S···S interaction within the Dawson $\{Mo^{VI}_{18}\}$ matrix is interesting since the formation of a dithionate anion would release two electrons to reduce the surrounding polyoxomolybdate shell to the mixed-valence reduction state $\{Mo^{VI}_{16}Mo^{V}_{2}\}$, with its characteristic blue color. Although switching has not yet been achieved, the sulfite-based clusters are thermochromic between 77 and 500 K [15].

By altering the synthetic conditions, it is also possible to obtain a sulfite-based polyoxotungstate, α-$[W_{18}O_{54}(SO_3)_2]^{4-}$ [16], which is isostructural with α-$[Mo_{18}O_{54}(SO_3)_2]^{4-}$ [14], and $[W^{VI}_{18}O_{56}(SO_3)_2(H_2O)_2]^{8-}$ [16]. The latter is described as a "Trojan horse" in which a structural rearrangement allows the two embedded pyramidal sulfite (SO_3^{2-}) anions to release up to four electrons (analogous to the "soldiers" hidden inside the "Trojan horse") to the surface of the cluster generating the sulfate-based, deep-blue, mixed-valence cluster $[W_{18}O_{54}(SO_4)_2]^{8-}$ upon heating (Figure 11.4). The sulfite anions adopt a radically different orientation in $[W^{VI}_{18}O_{56}(SO_3)_2(H_2O)_2]^{8-}$,

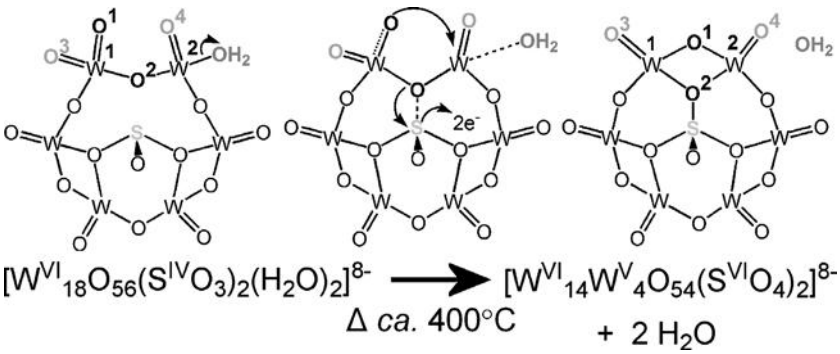

Figure 11.4 Scheme showing the change in the metal oxo framework on one half of the cluster upon oxidation of the internal SO_3^{2-} ligand to SO_4^{2-} (shown by the movement of each of the number oxygen atoms on the left to the end position on the right), which is commensurate with the reduction of the cluster shell by four electrons, giving rise to the deep-blue material from the colorless crystals.

whereby they each only ligate to seven metal centers: three from the cap and four (out of six) from the "belt" of the cluster framework.

The orientation for the sulfite anions within the cluster type is somewhat like the coordination mode for the tetrahedral templates (XO_4^{y-}) in conventional Dawson $[M_{18}O_{54}(XO_4)_2]^{2y-}$, i.e. one of the oxo ligand bridges three capping W centers, and the remaining oxo ligands each bridge two of the "belt" W centers. Nevertheless, this leaves two "belt" W atoms uncoordinated to the template SO_3 moiety as SO_3 has one oxo ligand less than XO_4. Hence it can be seen that the sulfite ions are grafted on to the bottom side of the cluster, which resembles a "basket" with four "uncoordinated" "belt" metal centers on the top part and now has a lower C_{2v} symmetry compared with the cluster α-$[Mo_{18}O_{54}(SO_3)_2]^{4-}$, which has a D_{3h} symmetry. To compensate for the coordination, these unique "uncoordinated" "belt" W centers (four for the whole cluster) each have two terminal ligands, rather than one as found for the remaining metal centers in the cluster. These are in addition to the four other μ_2 bridging oxo (O^{2-}) ligands between metal centers and complete a slightly distorted octahedral coordination geometry for each of the four "uncoordinated" "belt" metal centers concerned. Single-crystal structure analysis revealed that two of the four unique metal centers each have two W=O terminals (W−O ≈ 1.7 Å) and the other two each have one W=O terminal and one W−OH_2 terminal (W−O ≈ 1.7 and 2.2 Å, respectively). Furthermore, it is interesting that the unique "belt" μ_2 bridging oxo ligands between the pair "uncoordinated" "belt" W atoms now bends in towards the cluster, rather than outwards as normal, and is located ca. 2.9 Å distant from the sulfur center of the SO_3 moiety, whereas the two sulfur centers are positioned 3.6 Å apart at opposite sides of the cluster shell. In this respect, the mechanism for the reduction of the cluster shell requires an interaction between the sulfur atom and the special belt oxo ligand, which then react to form two sulfate anions located within the $\{W_{18}\}$ cluster shell.

In summary, compounds $[Mo_{18}O_{54}(SO_3)_2]^{4-}$ and $[W_{18}O_{56}(SO_3)_2(H_2O)_2]^{8-}$ demonstrate unprecedented electronic properties, thermochromism and a unique electron-transfer reaction, in which, when heated, a structural rearrangement allows the two embedded pyramidal sulfite ($S^{IV}O_3^{2-}$) anions to release up to four electrons to the surface of the cluster, generating the sulfate-based, deep-blue, mixed-valence cluster $[W_{18}O_{54}(SO_4)_2]^{8-}$. Although electron-transfer reactions and structural rearrangements are known for HPOMs, these electron transfer reactions are "confined" within a molecular nanocage whereby the electrons are "released" from the core of the cluster. Moreover, this property is really intriguing, from the point of view of nanoscience, and $[W_{18}O_{56}(SO_3)_2(H_2O)_2]^{8-}$ can be considered to be a prototype nanodevice which responds according to a stimulus.

11.4
Isopolyoxometalate Nanoclusters

Going one step further, someone could realize the fact that porosity, separation and ion transportation effects start being a noteworthy feature of the POM capsules.

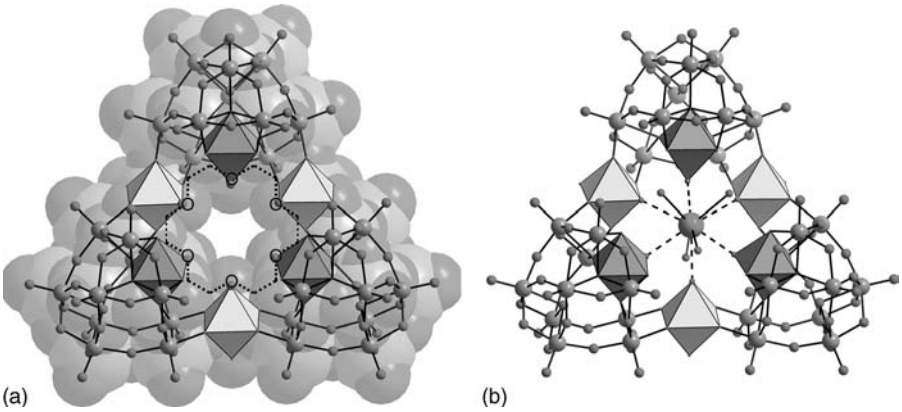

Figure 11.5 (a) Comparative illustration of the $\{W_{36}\}$ cluster framework $[H_{12}W_{36}O_{120}]^{12-}$ and the 18-crown-6 structure (show to scale). W and O atoms shown as light and dark spheres, respectively, with the crown ether superimposed on O atoms forming the "cavity" of the cluster. The ball and stick structure is also superimposed on the space-filling CPK representation, along with a polyhedral representation of the six W units that provide the "crown" coordinating O atoms. (b) The same ball and stick/polyhedral structure but this time showing the complexed potassium ion and the ligated water molecules within the cavity representing the overall $\{(H_2O)_4K\subset[H_{12}W_{36}O_{120}]\}^{11-}$ complex.

The $\{W_{36}\}$-based cluster with the formula $\{(H_2O)_4K_{[H_{12}}W_{36}O_{120}]\}^{11-}$ includes the threefold symmetric cluster anion $[H_{12}W_{36}O_{120}]^{12-}$ (Figure 11.5) [17]. The cluster anion complexes a potassium ion at the center of the $\{W_{36}\}$ cluster in an O_6 coordination environment. The $\{W_{36}\}$ structure consists of three $\{W_{11}\}$ subunits; these subunits contain a ring of six basal W positions, an additional W position in the center of this ring and four apical W positions in a butterfly configuration. Every W position around the cluster center has a distorted WO_6 octahedral coordination geometry with one terminal W=O moiety [d(W=O) ≈ 1.70 Å] extending towards the cluster center where the K ion is located; this arrangement maps extremely well on to the structure of the crown ether [18]crown-6.

The implications for the development of this system in a similar fashion to the crown ethers is interesting, especially the possibilities for discrimination and sensing of metal ions using this cluster framework [18]. The crown ether-like properties for the $\{W_{36}\}$ cluster can be realized in the presence of other cations such as K^+, Rb^+, Cs^+, NH_4^+ and Sr^{2+}, and it was determined that these ions can bind to the cluster and their structures crystallographically determined (Table 11.1).

As can be seen in the table, the found average oxygen–metal distances in the $\{W_{36}\}$ host–guest complexes **1**–**5** are very close to the distances shown in the corresponding 18-crown-6 complexes. The metal cations in the synthesized compounds show different distances to the equatorial plane of the cluster framework which reflect the different sizes of their ionic radii. Although there are some great similarities between the $\{W_{36}\}$ system and 18-crown-6, there are some features that are not common to both systems. First, the six-coordinated oxygen atoms on $\{W_{36}\}$ are not

Table 11.1 Comparison of acquired metal–oxygen distances and displacements of metal ions to the cavity center in the $\{W_{36}\}$ cluster and the corresponding figures for the 18-crown-6 ether (e.s.d.s are all with 0.02 Å).

		Average metal–oxygen distance (Å)		Distance from cavity center (Å)	
Cation	**Ionic radius (Å)**	**$\{W_{36}\}$ cluster**	**18-Crown-6**	**$\{W_{36}\}$ cluster**	**18-Crown-6**
K^+	1.38	2.80	2.80	0.70	0
Rb^+	1.52	2.87	2.95	0.84	0.93
Cs^+	1.67	3.16	3.18	1.61	1.47
Sr^{2+}	1.18	2.70	2.73	0.53	0
Ba^{2+}	1.35	2.82	2.82	0.73	0

planar, whereas those on 18-crown-6 can adopt a planar conformation. Further, the $\{W{=}O\}_6$ donor groups of the $\{W_{36}\}$ crown are rigid, unlike in 18-crown-6, which is much more flexible. This means that 18-crown-6 can deform to form metal complexes with small ions such as Na^+, Ca^{2+}, lanthanide ions and d-transition metal ions. This is because 18-crown-6, along with other similar crown ethers, is able to distort and wrap itself around these smaller metal cations in an attempt to maximize the electrostatic interactions. This increases the strain of the ligand, which makes these complexes less stable than those with metal cations of optimal spatial fit. However, the $\{W_{36}\}$ framework, due to its high rigidity, simply cannot change conformation in such a way as to bind these metal cations. This is partly confirmed by the observation that the diameter of the central cavity present in the family of $\{W_{36}\}$ clusters presented here is very well defined and rigid.

11.5 Keplerate Clusters

Reduced polyoxomolybdate clusters represent one of the most interesting cluster classes for nanoscience as these clusters adopt ring and spherical shapes comprising pentagonal $\{(Mo)Mo_5\}$ building blocks [5]. In particular, the spherical icosahedral $\{Mo_{132}\}$ Keplerate cluster as been described as an inorganic superfullerene due to its symmetry and large nanoscale size [19]. The discovery of such a cluster, particularly as it is spherical, water soluble and has such a large cavity, probably represents one of the most significant findings in recent years [20], especially since this discovery has gone on to reveal a whole family of related Keplerates. Within this family [20–33], all the spherical and approximately icosahedral clusters have the form $[\{(pent)_{12}(link)_{30}\}]$, e.g. like $[\{(Mo)(Mo_5O_{21}(H_2O)_6\}_{12}\{Mo_2O_4(ligand)\}_{30}]^{n-}$ with binuclear linkers where the 12 central pentagonal units span an icosahedron and the linkers form a distorted truncated icosahedron; the highly charged capsule with sulfate ligands and $n = 72$ was used very successfully. For instance, the truly nanoscale capsules (inner cavity diameter ca. 2.5 nm) allow different types of encapsulations, e.g. of well-structured

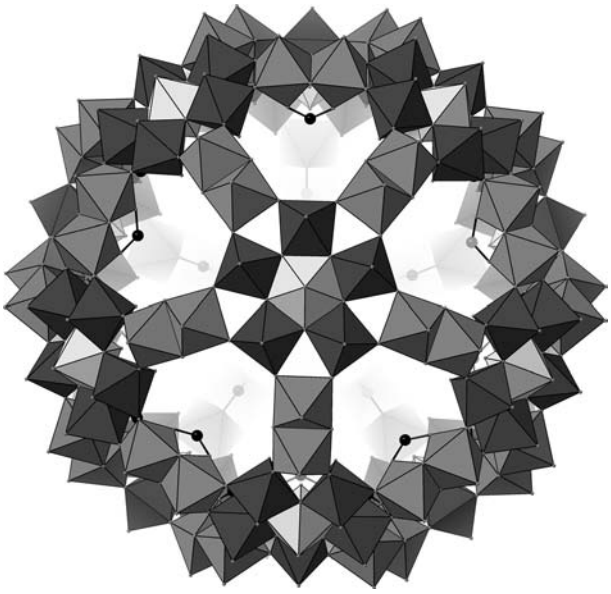

Figure 11.6 A polyhedral representation of the $\{Mo_{132}\}$ Keplerate cluster. The pentagonal $\{Mo_6\}$ building blocks and the $\{Mo_2\}$ building blocks can be seen. The bridgehead atom of the XO_2 bridge of the $\{Mo_2\}$ groups can be seen as black spheres.

large water assemblies (up to 100 molecules) with an "onion"-like layer structure enforced by the outer shell (Figure 11.6) [21]. Most importantly, the capsules have 20 well-defined pores and the internal shell functionalities can be tuned precisely since the nature of the bidentate ligands can be varied. In the special case of binuclear $Mo^{V}_{2}O_{4}^{2+}$ linkers the pores are $\{Mo_9O_9\}$ rings with a crown ether function (diameters 0.6–0.8 nm) which can be reversibly closed, e.g. by guanidinium cations interacting noncovalently with the rings via formation of hydrogen bonds [22]. In a related smaller capsule with mononuclear linkers, the $\{Mo_6O_6\}$ pores can become closed/complexed correspondingly by smaller potassium ions [23].

The most intriguing and exciting property of the highly negatively charged capsules is that they can mediate cation transfer from the solution to the inner nanocavity. Indeed, reaction of the above-mentioned highly charged capsule with different substrates/cations such as Na^+, Cs^+, Ce^{3+}, $C(NH_2)_3^+$ and $OC(NH_2)NH_3^+$ in aqueous solution leads to formations/assemblies which exhibit well-defined cation separations *at*, *above* or *below* the capsules channel-landscapes ("nano-ion chromatograph" behavior) [24]. Taking this one step further, a temperature-dependent equilibrium process that involves the uptake/release of Li^+ ions through the capsule pores has been observed: the porous capsule behaves as a semipermeable inorganic membrane open for H_2O and small cations [25,26]. Furthermore, the 20 pores of the same capsule "shut" by protonated urea as "stoppers" can be opened in solution, thus allowing calcium(II) ion uptake while later closing occurs again (Figure 11.7) [27]. Remarkably,

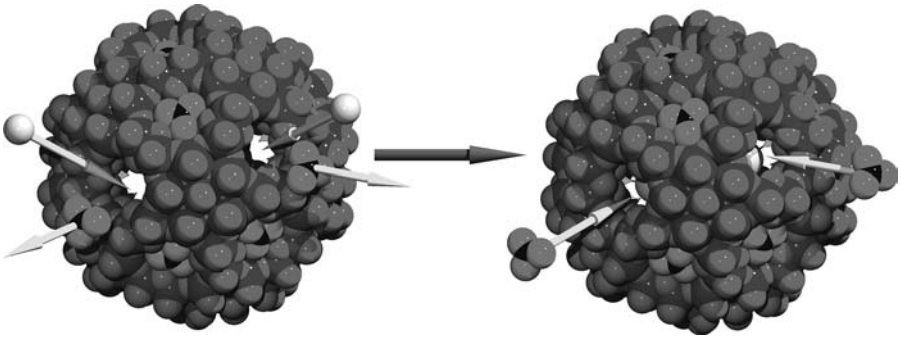

Figure 11.7 Space-filling representation demonstrating a simplified view of the Ca^{2+} ion uptake based on the capsule $[\{(Mo)(Mo_5O_{21}(H_2O)_6\}_{12}\{Mo_2O_4(SO_4)\}_{30}]^{72-}$. Initially the pores are closed, but treating a solution of the capsule with Ca^{2+} ions leads to cation uptake (left) while in the final product the pores again are closed (right; Mo, dark gray, O, medium gray, C, black, N/O(urea), light gray, Ca^{2+}, light gray spheres).

"pore gating" – just modeling biological ion transport – can illustratively be demonstrated: after initial cation uptake, subsequent cations are found hydrated above the pores due to a decrease of negative capsule charge [28].

This type of nanocapsules proved their efficiency in cation separation processes also in the presence of heavier metal atoms, such as Pr^{3+} [29]. The interesting phenomenon of metal cations such as Pr^{3+} entering into channels and the inner capsule, thereby constituting a novel situation with a metal center in two different environments corresponding to a coordination chemistry under confined conditions or, in other words, cation transfer in a controlled and specific fashion, has been reported. The reported findings open up perspectives for a special type of en capsulation chemistry, i.e. coordination chemistry under confined conditions. This can be extended to (1) a variety of ligands like the present one, (2) different capsule charges, (3) different types of porosity, (4) different solvent molecules like water and (5) different metal centers. In addition, the presence of cations such as Pr^{3+} in two different coordination geometries gives a unique opportunity to study the ligand influence on the electronic structure of rare earth compounds.

Furthermore, nanocapsules have given us also the opportunity to study the structures of the simplest chemical reagent we have in our hands, namely pure H_2O. Even though it is the simplest chemically known compound, it gives rise to a plethora of structural motifs which are difficult to study [30]. The use of nanocapsules as "crystallization flasks" has given the advantage of isolating different kinds of water structures, while the same system can also be studied as a probe to investigate "complex system" behavior in general, and further, a "new state of inorganic ions" involved in the formation of a novel type of aggregates [31], even allowing the control of the aggregate size by the change in the cluster charge. It is even possible to incorporate large cluster guests, e.g. $\{PMo_{12}O_{40}\}^{3-}$, within the Fe-substituted Keplerate cluster $\{Mo_{72}Fe_{30}\}$, where the Keplerate host acts rather like a prison, totally encompassing the guest or, more precisely, a hostage molecule to give

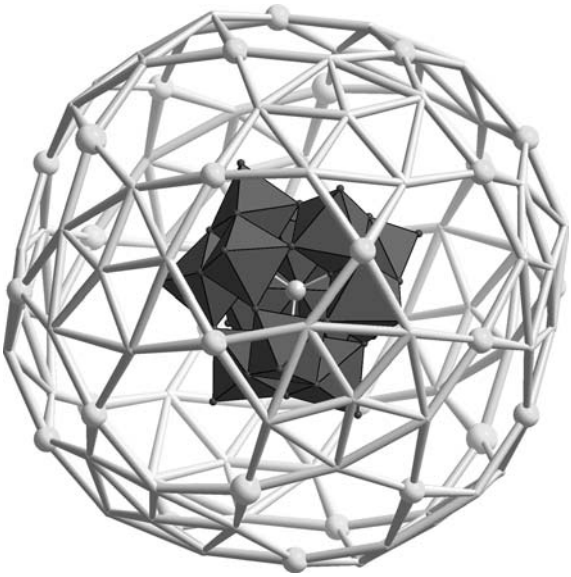

Figure 11.8 (a) Structure of $\{Mo_{12}\}\subset[\{Mo_{132}\}$. The hostage is shown in polyhedral form and the $\{Mo_{72}Fe_{30}\}$ is shown as the framework with the {Fe} positions shown as white spheres linking the 12 $\{(Mo^{VI})Mo^{VI}{}_5\}$ pentagons, and the Keggin nucleus in polyhedral representation.

the compound $[PMo_{12}O_{40\{(Mo^{VI})}Mo^{VI}{}_5\}_{12}Fe^{III}O_{252}(H_2O)_{102}(CH_3COO)_{15}].\sim 120H_2O$ (Figure 11.8) [32,33].

11.6
Surface-Encapsulated Clusters (SECs): Organic Nanostructures with Inorganic Cores

In an effort to combine inorganic polyoxometalates and organic materials chemistry, cationic surfactants have been applied to improve the surface properties of POMs. The resulting surfactant-encapsulated complexes (SECs) are compatible with organic matrixes, improve the stability of the encapsulated cluster against fragmentation, enhance the solubility in nonpolar, aprotic organic solvents and neutralize their charge, thus leading to discrete, electrostatically neutral assemblies, while altering the surface chemical properties in a predictable manner. Importantly, the basic physical and chemical properties of the polyoxometalates are retained [34] while the coexistence of hydrophobic alkyl chains and hydrophilic clusters in SECs gives them an amphiphilic character. Recently, it has been reported that this amphiphilic character is also exhibited in a solution environment and an unusual vesicular assembly of $(DODA)_4H$ $[Eu(H_2O)_2SiW_{11}O_{39}]$ (DODA = dimethyldioctadecylammonium) has been observed [35]. An even larger aggregation

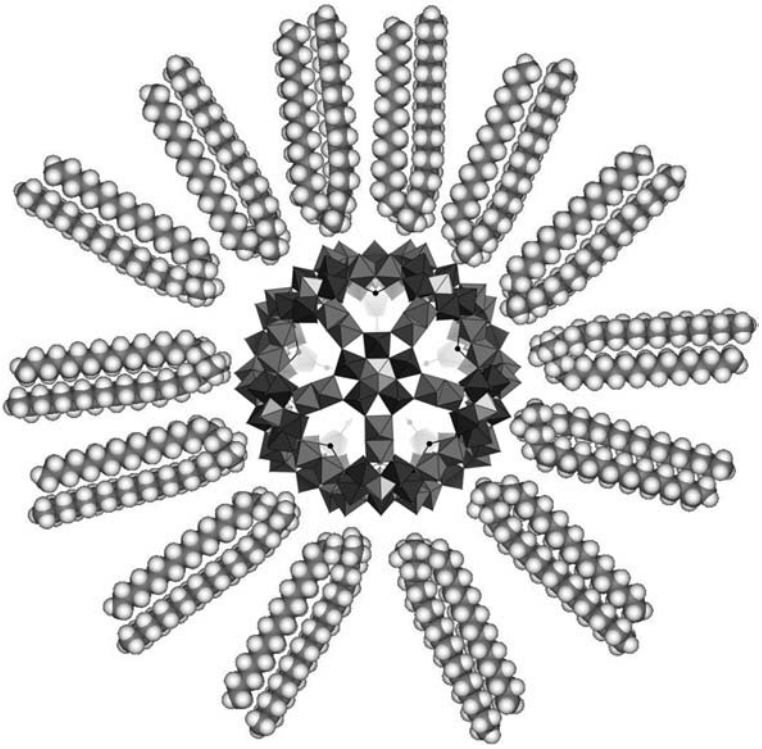

Figure 11.9 {Mo_{132}} SEC cluster $(DODA)_{40}(NH_4)_2$ $[(H_2O)_nMo_{132}O_{372}(CH_3CO_2)_{30}$ $(H_2O)_{72}]$ showing the inorganic core and the "soft" organic outer shell.

has been reported recently, the "onion"-like structure $(DODA)_4SiW_{12}O_{40}$ [36] and $(DODA)_{40}(NH_4)_2$ [$(H_2O)_nMo_{132}O_{372}(CH_3CO_2)_{30}$ $(H_2O)_{72}$] [37,38] (Figure 11.9) and also $(DODA)_{20}(NH_4)$ $[H_3Mo_{57}V_6(NO)_6O_{183}(H_2O)_{18}]$ [39], where the spherical species can provide a similar microenvironment to vesicles, which makes these assemblies suitable carriers to perform the catalytic and pharmacological functions of polyoxometalates. Moreover, the ability of polyoxometalates to undergo multiple reduction/oxidation steps may be exploited in information storage devices or optical switches. The possibility of fabricating well-defined two-dimensional arrays is an important step towards this goal.

The above-mentioned findings and suggestions reveal the feasibility of utilizing SECs as polyoxometalate-containing amphiphiles to construct regular assemblies from solution, help us to comprehend the catalyzing reactions of polyoxometalates in organic media, promote the effective interaction with organic molecules of biological interest and enhance, potentially, the interaction with biological media. However, the origin of the assembly process and whether it is a general behavior of SECs in solution are both still the subject of much debate and study.

11.7 Perspectives

It is clear that polyoxometalate-based building blocks can provide routes to the designed assembly of nanoscale capsules using coordinative interactions. This in turn is leading to and defining new areas of chemistry, i.e. under confined conditions, with parallels to processes/situations in biological cells regarding cell response and ion transport and even the possibility of engineering systems which exhibit complex and maybe adaptive behavior allowing chemical emergence. One tantalizing objective is the observation of evolving and dissipative inorganic systems. Generally, matter can be studied under confined conditions while the discovery of new systems resulting from encapsulation reveals new phenomena not observable in the bulk. This includes "confined water" with and without electrolytes and also spectacular chemical reactions. The presence of well-defined cavities/nanospaces and gated pores allows specific interactions of the capsules with their environments and subsequent uptake and selective binding of guests, since the architectures of the inner cluster walls can be "programmed/redesigned". Therefore, the design and synthetic approaches to polyoxometalates and the fact that these clusters can be constructed over multiple length scales, along with their almost unmatched range of physical properties, mean that they are serious candidates to be used as the functional part of any nano-device. The challenge now is to design individual POM cluster molecules that can interact both with each other and with the macroscale, in a desired fashion in response to inputs and environmental effects, so a functioning molecular system is really constructed. These capsule systems are truly fascinating and the future is exciting, since great leaps in understanding the principles that underpin the assembly mechanisms of such capsules allow the designed construction of extremely complex and specifically interacting systems – and this in the broadest sense is "bringing inorganic chemistry to life".

References

1 Sato, S., Iida, J., Suzuko, K., Kawano, M., Ozeki, T. and Fujita, M. (2006) *Science*, **313**, 1273.

2 Müller, A., Beckmann, E., Bögge, H., Schmidtmann, M. and Dress, A. (2002) *Angew. Chem. Int. Ed.*, **41**, 1162.

3 Pope M.T. and Muller A. (eds) (2001) *Polyoxometalate Chemistry: from Topology via Self-Assembly to Applications*, Kluwer, Dordrecht. Wassermann, K., Dickman, M.H. and Pope, M.T. (1997) *Angew. Chem. Int. Ed. Engl.*, **36**, 1445.

4 Long, D.-L., Burkholder, E. and Cronin, L. (2007) *Chem. Soc. Rev.*, **36**, 105.

5 Cronin, L. (2004) in *Comprehensive Coordination Chemistry II*, (eds J.A. McCleverty and T.J. Meyer), Vol. 7 Elsevier, Amsterdam, pp. 1–56.

6 Neumann, R. and Dahan, M. (1997) *Nature*, **388**, 353; Mizuno, N. and Misono, M. (1998) *Chem. Rev.*, **98**, 199.

7 Katsoulis, D.E. (1998) *Chem. Rev.*, **98**, 359; Yamase, T. (1998) *Chem. Rev.*, **98**, 307.

8 Rüther, T., Hultgren, V.M., Timko, B.P., Bond, A.M., Jackson, W.R. and Wedd, A.G. (2003) *J. Am. Chem. Soc.*, **125**, 10133.

9 Long, D.L., Kogerler, P., Parenty, A.D.C., Fielden, J. and Cronin, L. (2006) *Angew. Chem. Int. Ed.*, **45**, 4798.

10 Scheele, C.W. (1971) in *Sämtliche Physische und Chemische Werke*, (ed. D.S.F. Hermbstädt), M. Sändig, Niederwalluf/ Wiesbaden, Vol. 1 pp. 185–200 (reprint; original published 1783).

11 Müller, A., Krickemeyer, E., Meyer, J., Bögge, H., Peters, F., Plass, W., Diemann, E., Dillinger, S., Nonnenbruch, F., Randerath, M. and Menke, C. (1995) *Angew. Chem. Int. Ed.*, **34**, 2122.

12 Cronin, L., Diemann, E. and Müller, A. (2003) in: *Inorganic Experiments*, (ed. Woollins J.D.), Wiley-VCH, Weinheim, pp. 340–346.

13 Cronin, L., Beugholt, C., Krickemeyer, E., Schmidtmann, M., Bögge, H., Kögerler, P., Luong, T.K.K. and Müller, A. (2002) *Angew. Chem. Int. Ed.*, **41**, 2805.

14 Müller, A., Das, S.K., Talismanov, S., Roy, S., Beckmann, E., Bögge, H., Schmidtmann, M., Merca, A., Berkle, A., Allouche, L., Zhou, Y.S. and Zhang, L.J. (2003) *Angew. Chem. Int. Ed.*, **42**, 5039.

15 Long, D., Abbas, H., Kogerler, P. and Cronin, L. (2004) *Angew. Chem. Int. Ed.*, **43**, 1817.

16 Long, D., Abbas, H., Kogerler, P. and Cronin, L. (2005) *Angew. Chem. Int. Ed.*, **44**, 3415.

17 Long, D., Abbas, H., Kögerler, P. and Cronin, L. (2004) *J. Am. Chem. Soc.*, **126**, 13880.

18 Long, D.L., Brucher, O., Streb, C. and Cronin, L. (2006) *Dalton Trans.*, 2852.

19 Müller, A., Kögerler, P. and Bögge, H. (2000) *Struct. Bonding*, **96**, 203.

20 Müller, A., Krickemeyer, E., Bögge, H., Schmidtmann, M. and Peters, F. (1998) *Angew. Chem. Int. Ed.*, **37**, 3359.

21 Müller, A., Krickemeyer, E., Bögge, H., Schmidtmann, M., Botar, B. and Talismanova, M.O. (2003) *Angew. Chem. Int. Ed.*, **42**, 2085.

22 Müller, A., Krickemeyer, E., Bögge, H., Schmidtmann, M., Roy, S. and Berkle, A. (2002) *Angew. Chem. Int. Ed.*, **41**, 3604.

23 Müller, A., Botar, B., Bögge, H., Kögerler, P. and Berkle, A. (2002) *Chem. Commun.*, 2944.

24 Müller, A., Das, S.K., Talismanov, S., Roy, S., Beckmann, E., Bögge, H., Schmidtmann, M., Merca, A., Berkle, A., Allouche, L., Zhou, Y.S. and Zhang, L.J. (2003) *Angew. Chem. Int. Ed.*, **42**, 5039.

25 Müller, A., Rehder, D., Haupt, E.T.K., Merca, A., Bögge, H., Schmidtmann, M. and Heinze-Brückner, G. (2004) *Angew. Chem. Int. Ed.*, **43**, 4466.

26 Haupt, E.T.K., Wontorra, C., Rehder, D., Müller, A. (2005) *Chem. Commun.*, 3912. Müller, A., Botar, B., Bögge, H., Kögerler, P. and Berkle, A. (2002) *Chem. Commun.*, 2944.

27 Müller, A., Toma, L., Bögge, H., Schäffer, C. and Stammler, A. (2005) *Angew. Chem. Int. Ed.*, **44**, 7757.

28 Müller, A., Zhou, Y., Bögge, H., Schmidtmann, M., Mitra, T., Haupt, E.T.K. and Berkle, A. (2006) *Angew. Chem. Int. Ed.*, **45**, 460.

29 Müller, A., Zhoua, Y., Zhang, L., Bogge, H., Schmidtmann, M., Dresselb, M. and van Slageren, J. (2004) *Chem. Commun.*, 2038.

30 Müller, A., Krickemeyer, E., Bogge, H., Schmidtmann, M., Botar, B. and Talismanova, M.O. (2003) *Angew. Chem. Int. Ed.*, **42**, 2085.

31 Müller, A., Diemann, E., Kuhlmann, C., Eimer, W., Serain, C., Tak, T., Knoechel, A. and Pranzas, P.K. (2001) *Chem. Commun.*, 1928.

32 Müller, A., Das, S.K., Kögerler, P., Bögge, H., Schmidtmann, M., Trautwein, A.X., Schünemann, V., Krickemeyer, E. and Preetz, W. (2000) *Angew. Chem. Int. Ed.*, **112**, 3556.

33 Müller, A., Todea, A.M., Bogge, H., van Slageren, J., Dressel, M., Stammlera, A. and Rusuc, M. (2006) *Chem. Commun.*, 3066.

34 Tao, Y., Yu, Q. and Bu, X.H. (2007) *Chem. Commun.*, **15**, 1527.

35 Li, J.R., Bu, W., Li, H., Sun, H., Yin, S. and Wu, L. (2005) *J. Am. Chem. Soc.*, **127**, 8016.

36 Li, H., Sun, H., Qi, W., Xu, M. and Wu, L. (2007) *Angew. Chem. Int. Ed.*, **46**, 1300.

37 Kurth, D.G., Lehmann, P., Volkmer, D., Müller, A. and Schwahn, D. (2000) *J. Chem. Soc., Dalton Trans.*, 3989.

38 Kurth, D.G., Lehmann, P., Volkmer, D., Cölfen, H., Koop, M.J., Müller, A. and Chesne, A.D. (2000) *Chem. Eur. J.*, **6**, 385.

39 Volkmer, D., Chesne, A.D., Kurth, D.G., Schnablegger, H., Lehmann, P., Koop, M.J. and Müller, A. (1995) *J. Am. Chem. Soc.*, **46**, 122.

12
Nano-capsules Assembled by the Hydrophobic Effect

Bruce C. Gibb

12.1
Introduction

Compartmentalization is a key feature of living systems, helping to control in a temporal manner both where a particular molecule can be found, its concentration and what it can react with. This is in contrast to contemporary solution-based chemistry, where solvent, temperature and reactant concentrations offer some degree of control, but by and large random collision reigns. Moving from solution-based chemistry to systems that are compartmentalized in some manner therefore offers many exciting possibilities. Greater reaction control is one obvious example [1–5], but the complexity of biosystems undoubtedly harbors many as yet unknown "systems chemistry" phenomena that will only be pinpointed with the aid of model systems less complex than biochemical networks.

Compartments, of course, come in many shapes and sizes. They can be composed of a single shell-like molecule [6–9], but more often are engendered by the self-assembly of molecular subunits [10]. The nature of the subunits themselves determines what drives their assembly, whether the inner domain is similar or completely different from the outer domain, how thick the partition is (a few atoms, a bilayer, multiple bilayers?) and how permeable the shell or membrane is. Our focus here is a compartmentalization driven by the hydrophobic effect [11,12]. However, in contrast to "fluid" assemblies such as liposomes and micelles composed of many hundreds or thousands of copies of the subunits, the assemblies in question are dimerizations; dimers of bowl-shaped molecules called cavitands that are extremely well defined structurally (Figure 12.1). These assemblies also differ from micelles and liposomes in as much as a templating guest (or guests) is required to trigger assembly of the nano-capsule. Many analogous self-assembling systems have been reported previously, but the driving forces for their formation have been highly directional non-covalent forces such as hydrogen bonding [13–17] or metal

Organic Nanostructures. Edited by Jerry L. Atwood and Jonathan W. Steed

ISBN: 978-3-527-31836-0

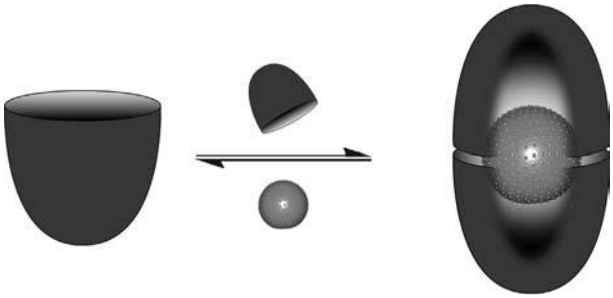

Figure 12.1 Cartoon of the dimerization of two cavitand molecules around a guest.

coordination [4,18–20]. Hence, the system in question offers a unique perspective on how the hydrophobic effect drives assembly and may shed light on biologically relevant assemblies such as protein quaternary structure.

12.2
Synthesis of a Water-soluble, Deep-cavity Cavitand

The structure of the water-soluble cavitand used to form the dimeric nano-capsules (**1**) is shown in Scheme 12.1. The synthesis is accomplished in seven steps, only two of which require purification by chromatography [21]. It begins with formation of the resorcinarene **2**, a reaction that can be performed easily on the hundreds of grams scale [22]. This resorcinarene is then converted to cavitand **3** by bridging using 3,5-dibromobenzal bromide; a compound available in near quantitative yields by treating the commercially available 3,5-dibromobenzaldehyde with BBr_3. Cavitand **3** is awkward to purify so without purification it is protected as its tetrabenzyl ether **4**. The 40% yield for the two steps understates the efficiency of the initial stereoselective bridging that forms four stereogenic centers and eight covalent bonds. Thus, assuming quantitative protection, a 40% yield corresponds to an average 89% yield for each bond formed and an average diastereoselectivity of 80% for each stereogenic center. Subsequently, octabromide **4** is treated with commercially available 3,5-dihydroxybenzyl alcohol to yield, after an eight-fold Ullmann ether reaction, cavitand **5**. Again, the 40% yield for this reaction understates the efficiency of this process; each aryl ether bond is formed in an average 89%. Finally, removal of the benzyl groups and oxidation give octa-acid cavitand **1** in quantitative yield.

12.2.1
Structure of the Cavitand (What It Is and What It Is Not)

A space-filling model of cavitand **1** is shown in Figure 12.2a. The molecule is in essence a curved amphiphile. It has a hydrophobic concave surface and a hydrophilic convex surface. The former defines a pseudo-conical cavity approximately 1 nm in diameter and 1 nm in depth, whereas the latter is decorated with eight carboxylic acid

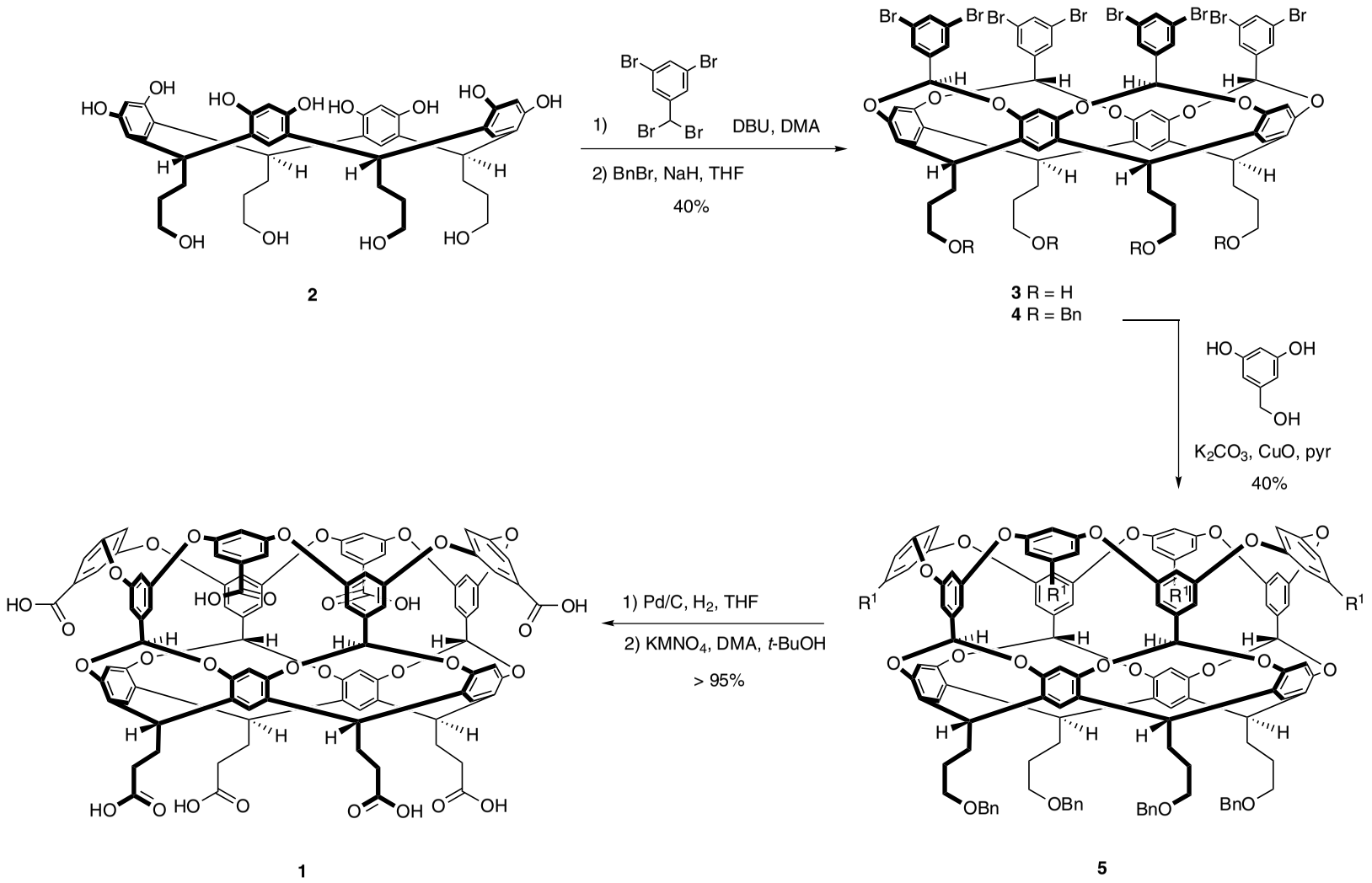

Scheme 12.1 Synthesis of octa-acid cavitand **1**.

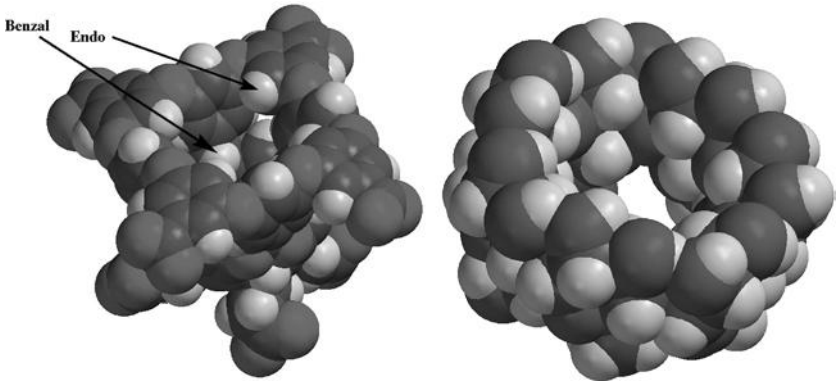

Figure 12.2 Space-filling models of (a) the octa-carboxylate of cavitand **1** and (b) β-cyclodextrin.

groups. This functionality bestows cavitand **1** with sparing water solubility at pH 7, but considerable solubility in basic solutions. Three other structural features should be mentioned. First, what is parochially termed the third row of aromatic rings – those introduced during the Ullmann ether reaction – define a wide hydrophobic rim. It is this rim that acts as an interface between the subunits of the nanocapsule. Second, the cavitand has only one significant portal. There is a small hole at the base of the cavity, but models suggest that it can only act as a portal for small diatoms traveling along the C_4 axis of the host. Essentially the cavity is closed at its base. Third, there are two kinds of H atoms that point into the cavity: the benzal (or acetal) hydrogens near the base of the cavity and what are termed the endo hydrogens (Figure 12.2a). Both are sensitive to guest binding, especially if the guest is halogenated (the guest will form hydrogen bonds with the benzal hydrogens) or a capsule is formed (the endo atoms become part of the interface).

Compare these structural features with β-cyclodextrin (Figure 12.2b). Like cavitand **1**, β-cyclodextrin has a cavity about 1 nm wide. At this point, however, the similarities end. The truncated conical cavities of cyclodextrins are so foreshortened that they are essentially tori; they are open at both ends, giving them a bangle-like structure that automatically diminishes the significance of dissociative mechanisms of guest exchange. Furthermore, both rims of the cyclodextrins are decorated with hydroxy groups. Hence, cyclodextrins are predisposed [23] to form 1:1 complexes in aqueous solution [24], and persuading them to do otherwise requires either a guest of specific shape and rigidity or modification to the cyclodextrins themselves. In summary, although both are water-soluble hosts with cavities about 1 nm in diameter, there are few structural features common to cavitand **1** and β-cyclodextrin.

12.2.2
Assembly Properties of the Cavitand

At relatively low concentrations (~1 mM), NMR spectroscopy confirms that cavitand **1** is monomeric [21]. Thus, the ^{1}H NMR spectrum of the host in sodium tetraborate

buffer shows sharp signals for each H atom, while diffusion rate measurements [25] with pulse gradient spin echo (PGSE) NMR reveals a molecule about 8 nm^3 in volume. In contrast, at higher concentrations (~20 mM), the ^1H NMR spectrum of the host shows exceptionally broad signals indicative of aggregation. This result was, to a degree, expected. One of the central theses of this program is to determine the degree of predisposition [23] required for a molecule to assemble via the hydrophobic effect and we had assumed that, without highly complementary and preorganized guests (templates), assembly to a well-defined dimer would not occur. Our line of thinking was as follows: if an interface between subunits involves highly directional noncovalent forces such as hydrogen bonds or metal coordination, the precise form of the assembled product is intimately tied to its enthalpy of formation. But what if the interfacial forces are weak and non-directional, such as the presupposed π–π stacking and C−H···π interactions in the dimer of **1** (Figure 12.3)? [26]. In other words, what if the assembly is instead driven by entropy? Can the hydrophobic effect lead to discrete assemblies of molecules possessing relatively small and topologically mundane interfaces? The analogy from Nature is, of course, protein quaternary structure [27], with the most exquisite examples perhaps being viral capsids [28]. By and large. however, the protein–protein interfaces (or hot-spots) are of the order of 600 $Å^2$ and highly complementary in terms of both their shape and distribution of functionality.[29] In contrast, the rim of cavitand **1** amounts to between 100 and 200 $Å^2$ of rather flat, uninspiring interface. As it transpires, our concerns were unfounded: cavitand **1** is highly predisposed – verging on

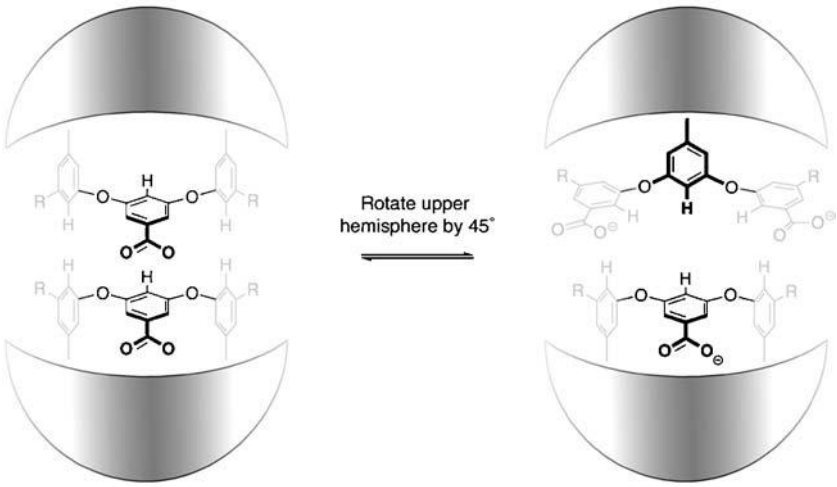

Figure 12.3 Schematic of the capsule interface. It is presumed that the two hemispheres can readily rotate around their common C_4 axis. If the two hemispheres are in register, face-to-face π–π-stacking dominates (left), whereas when out of register by 45° two kinds of C–H···π interactions are possible.

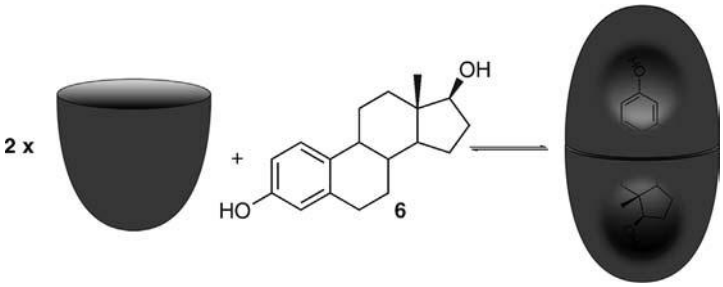

Figure 12.4 Self-assembly of **1** and encapsulation of estradiol (**6**).

"trigger happy" – to undergo assembly. It surpassed our initial expectations with consummate ease.

Our first encapsulation targets were steroids, primarily because molecules such as estradiol (**6**, Figure 12.4) appeared to be complementary in shape to the capsule, in addition to being hydrophobic. Additionally, however, their low symmetry (C_1) would help in confirming assembly [21]. As expected then, when estradiol was sonicated with a solution of cavitand **1**, the steroid was quickly taken up into solution.

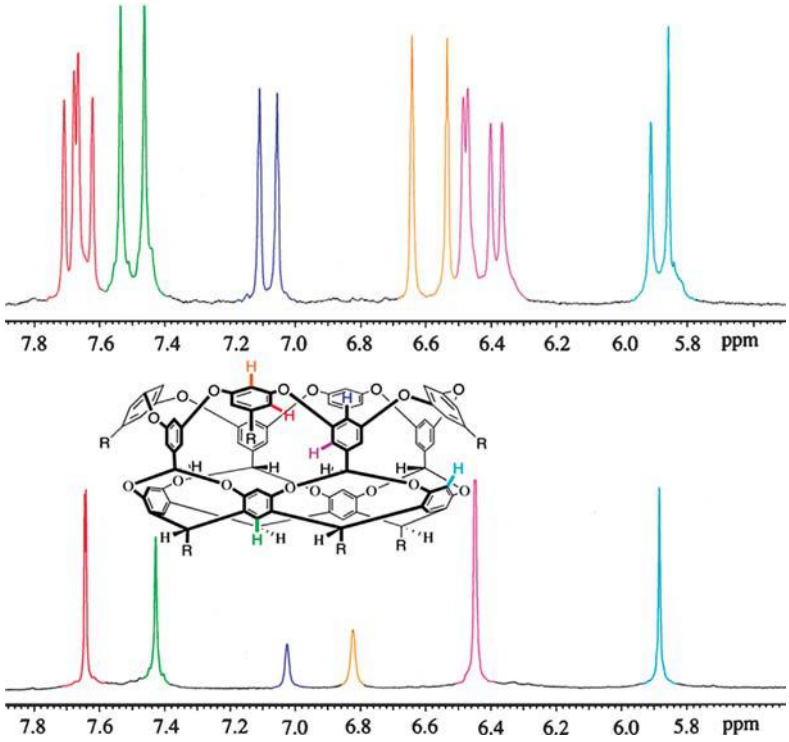

Figure 12.5 Selected region of the ^{1}H NMR spectrum of cavitand **1** (lower trace) and its 2:1 complex with estradiol **6** (upper trace).

NMR spectroscopy clearly showed capsule formation (Figure 12.5). Because the A and D rings of the steroid are aromatic and aliphatic, respectively, encapsulation resulted in two magnetically dissimilar "hemispheres". Consequently, as the exchange between free and bound guest was slow on the NMR time-scale, this led to a doubling of all signals from H atoms proximal to the guest, including the endo hydrogens (orange, Figure 12.5). In addition, though, the H atoms that were enantiotopic in the achiral free host (e.g. blue in Figure 12.5) became diastereotopic in the chiral complex. Consequently, these signals were doubled again. Encapsulation was also evident in the position of the bound guest signals. As expected, these were shifted upfield relative to their free position (in DMSO) because they experience magnetic shielding from the shell of the host. In particular, those guest atoms that were necessarily positioned towards the "poles" of each hemisphere underwent the largest shifts. Finally, capsule formation was also evident from NOESY NMR experiments. These revealed not only NOE interactions between the interface hydrogens of the two hemispheres, but also interactions between each end of the guest and the inward pointing benzal hydrogens of the host.

Estradiol was not actually the best guest for the capsule. Of the eight steroids examined, dehydroisoandrosterone (**7**) fitted best. In competition experiments it displaced estradiol, presumably because its more voluminous A-ring and C-18 methyl group filled the cavity of **1** better than an aromatic ring. One of the poorest guests examined was cholesterol (**8**), which although solubilized by the cavitand, did not yield a kinetically stable (500 MHz NMR time-scale) capsule. Models indicate that with its long C-17 chain, this guest was slightly too large for the capsule. As a result, the two hemispheres could not clamp down on one another to form a tight, desolvated interface.

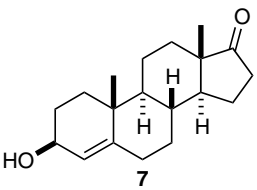

7

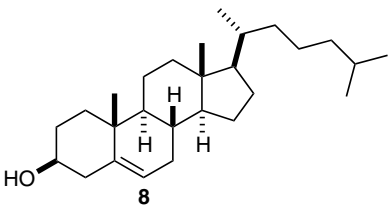

8

Having demonstrated successful capsule formation, our next task was to determine how preorganized the guest needed to be to form a well-defined capsule. We opted to dive in at the deep-end and study straight-chain alkanes [30]. How less preorganized can you get! The availability of a large number of alkanes in this homologous series offered a detailed analysis of the assembly properties of the cavitand and the carrying capacity of the capsule; the macro-scale equivalent to seeing how many methylene groups can be fitted into a cavity is the use by some car manufacturers of cubes of a defined size to estimate the volume of a trunk (boot). We examined the potential guests pentane through octadecane. Only the latter appeared not to form a stable complex with **1**. For the other molecules, the ^{1}H NMR spectra indicated that the smaller guests formed complexes with a host to guest ratio of 1 : 1,

Table 12.1 Summary of the complexes formed by **1** with straight-chain alkanes.

Guest	Ternary complex?	Quaternary complex?	Molecular formula of contents	Percentage occupancy[a]
Pentane	√	×	$C_{10}H_{24}$	43
Hexane	√	×	$C_{12}H_{28}$	50
Heptane	√	×	$C_{14}H_{32}$	57
Octane	√	√	$C_8H_{18}/C_{16}H_{36}$	33/65
Nonane	×	√	C_9H_{20}	36
Decane	×	√	$C_{10}H_{22}$	40
Undecane	×	√	$C_{11}H_{24}$	43
Dodecane	×	√	$C_{12}H_{26}$	47
Tridecane	×	√	$C_{13}H_{28}$	50
Tetradecane	×	√	$C_{14}H_{30}$	54
Pentadecane	×	√	$C_{15}H_{32}$	58
Hexadecane	×	√	$C_{16}H_{34}$	62
Heptadecane	×	√	$C_{17}H_{36}$	65

[a] These values assume a capsule volume of ~500 Å^3. However, defining what is termed usable space is highly subjective. Given free reign, workers in the laboratory have estimated cavity volumes from 400 to 700 Å^3. 500 Å^3 therefore is therefore on the conservative side of the average value obtained (600 Å^3).

whereas larger guests formed 2:1 entities. However, PGSE experiments revealed that the former had a stoichiometry of 2:2 rather than 1:1. In other words, small guests such as pentane formed quaternary capsular complexes with two entrapped guests. Table 12.1 summarizes the complexes formed and the percentage occupancy in each complex. From an admittedly biased standpoint, the fact that guests as small as pentane template capsule formation is remarkable; two small molecules, occupying less than half the volume of the capsule, are capable of templating its formation. Even though only weak C−H···π and/or π−π stacking forces exist within the interface (Figure 12.3) and between hosts and guests, a kinetically stable complex is formed.

Octane is a unique guest; on the cusp between ternary and quaternary complexes it forms both. Although it was not possible to "visualize" these two complexes directly with NMR, it was possible to infer this by examining shift data for the endo hydrogens of the host as a function of total guest volume. With the exception of octane, all the host–guest complexes formed two distinct trends for the ternary and quaternary entities. If it was assumed that octane formed a ternary complex, its shift data suggest a much larger guest, whereas if a quaternary complex was assumed, the shift corresponded to a much smaller guest. This observation is best explained by simultaneously invoking both ternary and quaternary complexes. As a result of this duality, octane covers the gamut of binding in terms of the total volume of the guest(s) or the percentage occupancy.

CPK models demonstrated that guests larger than roughly decane cannot reside in the capsule in a fully extended conformation, a point previously noted by Rebek and coworkers for analogous hydrogen bonded capsules [31,32] where long alkanes preferentially adopt helical conformations. We therefore used NOESY NMR to look

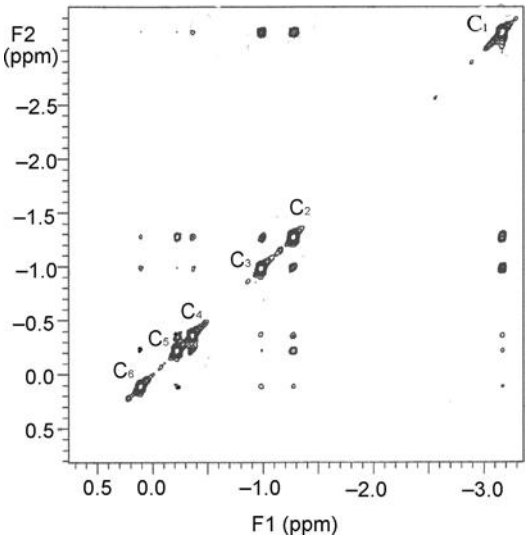

Figure 12.6 Section of the NOESY NMR spectrum of the dodecane complex with cavitand **1**.

for tell-tail signs that the guests inside the capsule formed by **1** also adopted preferred conformations. These studies revealed that only for guests larger than dodecane were 1,3 and 1,4 interactions indicative of helical structure observed (Figure 12.6), but the latter were rather weak, suggesting that a helical conformation was at best only marginally preferred. What is the difference between the capsules here and the related capsules of Rebek and coworkers? We suspect that the capsule $\mathbf{1}_2$ is slightly wider and therefore is not an ideal template for promoting helix formation.

12.2.3
Photophysics and Photochemistry Within Nano-capsules

We will return to the properties of these capsules and how the hydrophobic effect can promote unusual binding phenomena and separations. In the interim, it is also worth highlighting our collaboration with Ramamurthy's and Turro's groups, where we examine how photochemical or photophysical processes carried out inside the capsule differ from their counterparts in free solution. These experiments not only reveal how photochemical processes can be made more selective and suggest new ways in which organic chemistry can be brought into aqueous solution, but also shine light on the relatively unexplored phenomenon of external or concave templation. This type of templation, where the template is the host rather than the more typical guest, lags behind its more familiar counterpart because of the size requirement of the template; they need to be large enough to encapsulate interesting guests. That said, they should not be so large that guests never encounter the walls of the reaction vessel, for in an extreme case of a capsule filled with many guests, the center of these will resemble the liquid or solution state.

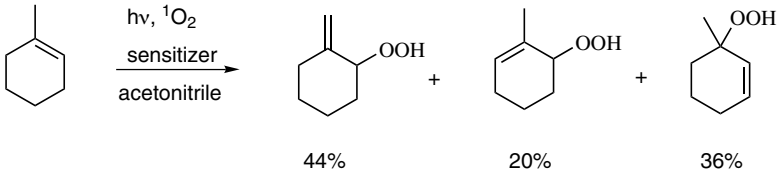

Scheme 12.2 Oxidation of 1-methylcyclohexene with singlet oxygen.

We have published on how the capsule formed by **1** can (1) redirect the Norrish Type I reactivity of dibenzyl ketones to give rearrangement products not observed in solution [33], (2) template the formation of the notoriously difficult to observe anthracene excimer [34] and (3) constrain the photo-Fries reactivity of naphthyl esters to one product instead of the more normal nine [35].

Most recently, we have reported on the reaction between singlet oxygen ($^1O_2$) and encapsulated alkenes [36]. In solution, the regioselectivity of this reaction is poor for substrates with multiple allylic hydrogens (Scheme 12.2) and so we wished to examine whether encapsulation could enhance selectivity. In addition, however, this particular reaction also raises the bar in terms of (encapsulated) reaction complexity. Is a water-soluble sensitizer required or can one be bound within a capsule? Also, can oxygen enter the capsule(s) containing the substrate (and sensitizer)? As it transpires, oxygen migration is not an issue, whether the sensitizer is water-soluble Rose Bengal or encapsulated dimethylbenzil (DMB) (Scheme 12.3). In either case, substrate encapsulation leads to highly regioselective reaction, although the reaction kinetics are slower if the sensitizer is encapsulated.

Whereas only one copy of DMB fits within the capsule formed by **1**, two copies of substrates such as 1-methylcyclohexene (MCH) occupy the host. NMR demonstrated that all of the methylcycloalkenes examined adopted one principal orientation in which the methyl group fills the tapering end of a cavity (Scheme 12.3). NMR also showed that mixing solutions of the two kinds of capsules did not result in guest exchange and the formation of capsules containing one DMB molecule and one substrate.

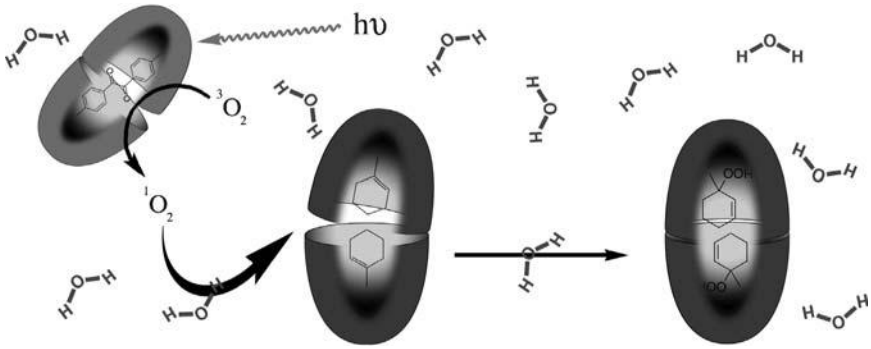

Scheme 12.3 Capsular control of the oxidation of 1-methylcyclohexene.

With this information at hand, we examined the outcome of irradiating (at 310 nm) the mixed solutions. That upon excitation encapsulated DMB generated $^1O_2$ was evident from the characteristic phosphorescence emission of $^1O_2$ at 1270 nm. An analysis of the quenching of the DMB as a function of $[O_2]$ gave a rate for this "bimolecular" energy transfer one order of magnitude less than for diffusion, but four orders of magnitude greater than the rate of energy transfer to O_2 from biacetyl triplet encapsulated in a covalent capsule [37]. Furthermore, kinetic traces of the phosphorescence of DMB and $^1O_2$ monitored at 560 and 1270 nm, respectively, revealed a 30-μs lag (rise time) between excitation of DMB and maximal $^1O_2$ phosphorescence, indicating that oxygen is not automatically present in the DMB capsule, but has to work its way in to undergo excitation. Once excited, however, the $^1O_2$ is free to enter other capsules and if one of these contains substrate, only one of the three allylic positions (the 3-position) undergoes hydrogen abstraction. Consequently, excellent yields of the corresponding tertiary hydroperoxide are obtained. We do not know the full details of this mechanism of attack and indeed there are still many things that we do not understand about the overall system. However, it is evident that capsule $\mathbf{1}_2$ can successfully bring about fairly complex reactions in which a reagent can move between two different capsules. We are therefore interested in examining further this approach to organic chemistry in water.

12.2.4
Hydrocarbon Gas Separation Using Nano-capsules

We finish this short review by returning to hydrocarbon binding within $\mathbf{1}_2$ with a twist, a twist that highlights the remarkable ability of **1** to self-assemble into discrete capsules and illustrates a unique way to separate hydrocarbon gases [38].

Our first attempt to bind hydrocarbon gases simply involved the bubbling of butane gas through a buffered, aqueous solution of **1**. Peak shifts for the endo and benzal hydrogen signals that point into the cavity indicated complexation, but there was only a broad signal in the high-field region of the NMR spectrum that could be attributed to bound guest (Figure 12.7a and b). However, these bound guest signals sharpened when the excess butane was allowed to escape from solution (Figure 12.7c). Integration of this kinetically stable complex confirmed a 1:1 ratio of host to guest, but it again took a PGSE experiment to reveal that the stoichiometry was 2:2 and that we were dealing with a stable capsular complex.

If binding is fairly strong, then it should be possible to extract a gas directly from the gas phase. This was shown in a subsequent experiment in which without agitation the quaternary butane complex formed spontaneously. Likewise, propane was also shown to template the formation of the capsule via direct extraction from the gas phase. In contrast to butane and propane, PSGE experiments reveal that ethane only formed a 1 : 1 complex. Apparently, the templation limit for the capsule is propane, at least in solutions devoid of salts known to increase the hydrophobic effect. In solutions of 14 mM NaCl, butane binding has been observed to be nearly two orders of magnitude greater than in NaCl-free solutions [39]. Hence ethane may ultimately be able to template the formation of the capsule. That point aside, that propane can

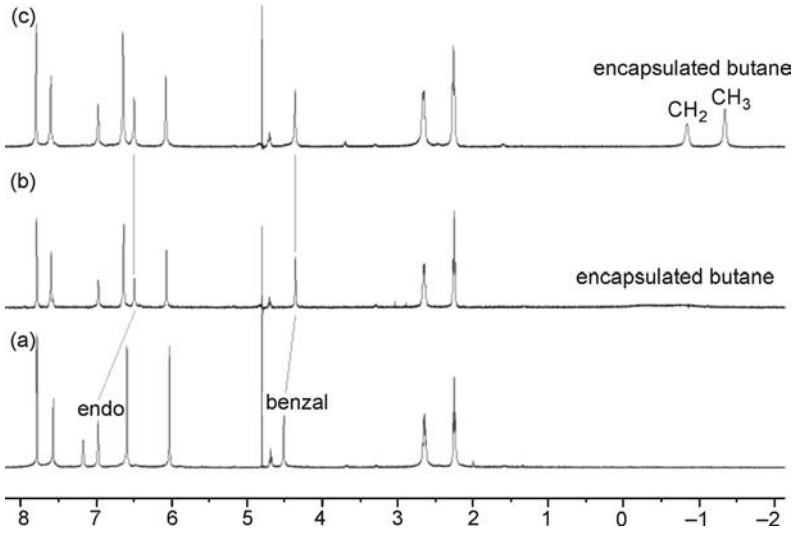

Figure 12.7 ^{1}H NMR spectra of (a) the free host, highlighting the signals from the endo and benzal hydrogens, (b) the 2 : 2 complex formed between **1** and excess butane and (c) the 2 : 2 complex of **1** and butane formed by extraction of the hydrocarbon gas directly from the gas phase.

template capsule formation is surprising. When we originally set out to synthesize cavitand **1**, we did not assume that its assembly would be templated by something as small as propane, a guest that results in complexes with an occupancy of 28%. There could be a host deformation that tempers this low value somewhat, but if the pocket is reduced in volume then the pressure of the contents increases; which is problematic because assuming a maximal cavity, (näve) calculations treating the guest as ideal give an internal pressure of 100 atm!

In these experiments, it was noted that propane binding was weaker than that of butane. Consequently, we decided to determine whether an aqueous solution of **1** could be used to separate these gases. We formed a mixture of the two hydrocarbons and exposed a large excess (to give relatively rapid uptake in the absence of agitation) to an aqueous solution of the host. As expected, NMR revealed that only the butane complex was formed, giving a gas phase mixture enriched in propane. As hydrocarbon gases cannot yet be separated by membrane technologies, capsule $\mathbf{1}_2$ suggests some interesting alternative strategies.

12.3 Conclusions

We have been surprised by the predisposition of cavitand **1** to self-assemble into a dimeric capsule. Two anthracene molecules can template capsule formation packing the cavity to about an 80% occupancy ratio; two propane molecules (~28% occupancy)

can do likewise. The tenacity of the hydrophobic effect is sufficient to allow the capsule to act as an external template and bring about unusual reactions and prevent the capsule from "blowing its own top" when filled with hydrocarbon gas. Nevertheless, these capsular assemblies are dynamic, reversibly formed entities. An interjection is required at this point. What do we mean by the hydrophobic effect? There are, after all, several flavors. Our early thermodynamic analyses suggest a nonclassical hydrophobic effect (ΔH° negative, ΔS° small) driving the formation of 1:1 complexes and a classic hydrophobic (ΔH° small, ΔS° positive) effect driving capsule capping. Furthermore, it seems that generally $K_1 < K_2$). More studies are needed to confirm these points, but with an assembly primarily driven by entropy we should repeat the question posed earlier: how can the hydrophobic effect lead to discrete assemblies with molecules with relatively small and topologically mundane interfaces? Towards answering these and other questions, we are continuing to investigate the subtleties behind these assemblies and the properties of the resulting complexes.

Acknowledgement

The author gratefully acknowledges the National Institutes of Health for financial support (GM074031).

References

1 Leung, D.H., Bergman, R.G. and Raymond, K.N. (2007) *J. Am. Chem. Soc.*, **129**, 2746–2747.
2 Kang, J. and Rebek, J. Jr. (1997) *Nature*, **385**, 50–52.
3 Heinz, T., Rudkevich, D.M. and Rebek, J.J. (1998) *Nature*, **394**, 764–766.
4 Fujita, M., Tominaga, M., Hori, A. and Therrien, B. (2005) *Acc. Chem. Res.*, **38**, 371–380.
5 Yoshizawa, M., Tamura, M. and Fujita, M. (2006) *Science*, **312**, 251–254.
6 Cram, D.J. and Cram, J.M. (1994) *Container Molecules and Their Guests*, 1st edn., Royal Society of Chemistry, Cambridge.
7 Liu, X., Liu, Y., Li, G. and Warmuth, R. (2006) *Angew. Chem. Int. Ed.*, **45**, 901–904.
8 Warmuth, R. and Yoon, J. (2001) *Acc. Chem. Res.*, **34**, 95–105.
9 Warmuth, R. (2001) *Eur. J. Org. Chem.*, 423–437.
10 MacGillivray, L.R. and Atwood, J.L. (1999) *Angew. Chem. Int. Ed.*, **38**, 1018–1033.
11 Chandler, D. (2002) *Nature*, **417**, 491.
12 Tanford, C. (1980) *The Hydrophobic Effect. Formation of Micelles and Biological Membranes*, 2nd edn., Wiley, New York.
13 Hof, F. and Rebek, J. Jr. (2002) *Proc. Natl. Acad. Sci. USA*, **99**, 4775–4777.
14 Rebek, J. Jr. (2005) *Angew. Chem. Int. Ed.*, **44**, 2068–2078.
15 MacGillivray, L.R. and Atwood, J.L. (1997) *Nature*, **389**, 469–472.
16 Atwood, J.L., Barbour, L.J. and Jerga, A. (2002) *Proc. Natl. Acad. Sci. USA*, **99**, 4837–4841.
17 McKinlay, R.M., Thallapally, P.K. and Atwood, J.L. (2006) *Chem. Commun.*, 2956–2958.
18 Fujita, M., Umemoto, K., Yoshizawa, M., Fujita, N., Kusukawa, T. and Biradha, K. (2001) *Chem. Commun.*, 509–518.

19 Caulder, D.L. and Raymond, K.N. (1999) *J. Chem. Soc., Dalton Trans.*, 1185–1200.
20 Davis, A.V., Yeh, R.M. and Raymond, K.N. (2002) *Proc. Natl. Acad. Sci. USA*, **99**, 4793–4796.
21 (a) Gibb, C.L.D. and Gibb, B.C. (2004) *J. Am. Chem. Soc.*, **126**, 11408–11409. (b) for a recent review on water-soluble cavitand, see Biros, S. and Rebek, J. Jr. (2007) *Chem. Soc. Rev.*, **36**, 93–104.
22 Gibb, B.C., Chapman, R.G., Sherman, J.C. (1996) *J. Org. Chem.*, **61**, 1505–1509.
23 Rowan, S.J., Hamilton, D.G., Brady, P.A. and Sanders, J.K.M. (1997) *J. Am. Chem. Soc.*, **119**, 2578–2579.
24 Rekharsky, M.V. and Inoue, Y. (1998) *Chem. Rev.*, **98**, 1875–1917.
25 Cohen, Y., Avram, L. and Frish, L. (2005) *Angew. Chem. Int. Ed.*, **44**, 520–554.
26 Meyer, E.A., Castellano, R.K. and Diederich, F. (2003) *Angew. Chem. Int. Ed.*, **42** , (11), 1210–1250.
27 Petsko, G.A. and Ringe, D. (2004) *Protein Structure and Function*, New Science Press, London.
28 Casper, D.L.D. and Klug, A. (1962) *Symp. Quant. Biol.*, **27**, 1–24.
29 Peczuh, M.W. and Hamilton, A.D. (2000) *Chem. Rev.*, **100**, 2479–2494.
30 Gibb, C.L.D. and Gibb, B.C. (2007) *Chem. Commun.*, 1635–1637.
31 Scarso, A., Trembleau, L. and Rebek, J. Jr. (2004) *J. Am. Chem. Soc.*, **126**, 13512–13518.
32 Scarso, A., Trembleau, L. and Rebek, J. Jr. (2003) *Angew. Chem. Int. Ed.*, **42**, 5499–5502.
33 Kaanumalle, L.S., Gibb, C.L.D., Gibb, B.C. and Ramamurthy, V. (2004) *J. Am. Chem. Soc.*, **126**, 14366–14367.
34 Kaanumalle, L.S., Gibb, C.L.D., Gibb, B.C. and Ramamurthy, V. (2005) *J. Am. Chem. Soc.*, **127**, 3674–3675.
35 Kaanumalle, L.S., Gibb, C.L.D., Gibb, B.C. and Ramamurthy, V. (2007) *Org. Biomol. Chem.*, **5**, 236–238.
36 Natarajan, A., Kaanumalle, L.S., Jockusch, S., Gibb, C.L.D., Gibb, B.C., Turro, N.J. and Ramamurthy, V. (2007) *J. Am. Chem. Soc.*, **129**, 4132–4133.
37 (a) Balzani, V., Pina, F.A., Parola, J., Ferreira, E., Maestri, M., Armaroli, N. and Ballardini, R. (1995) *J. Phys. Chem.*, **99**, 12701–12703. (b) Farran, A. and Deshayes, K. (1996) *J. Phys. Chem.*, **100**, 3305–3307. (c) Place, I., Farran, A., Deshayes, K. and Piotrowiak, P. (1998) *J. Am. Chem. Soc.*, **120**, 12626–12633.
38 Gibb, C.L.D. and Gibb, B.C. (2006) *J. Am. Chem. Soc.*, **128**, 16498–16499.
39 Gibb, C.L.D. and Gibb, B.C., unpublished work.